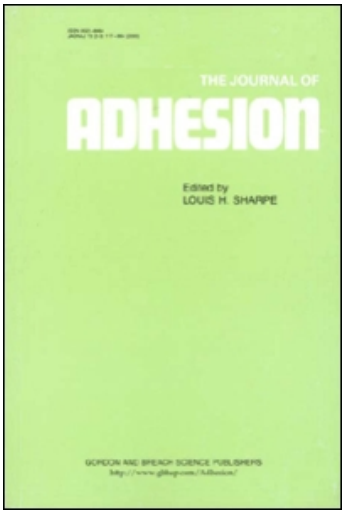

The Journal of Adhesion
Publication details, including instructions for authors and subscription information:
http://www.informaworld.com/smpp/title~content=t713453635

Creep Behaviour at High Temperature of Epoxy-imide/Steel Joints - Influence of Environment on Creep Rate

N. Piccirelli[a]; Y. Auriac[a]; M. E. R. Shanahan[a]
[a] Centre National de la Recherche Scientifique, Ecole Nationale Supérieure des Mines de Paris, Centre des Matériaux P.M. Fourt, EVRY Cédex, France

To cite this Article Piccirelli, N. , Auriac, Y. and Shanahan, M. E. R.(1998) 'Creep Behaviour at High Temperature of Epoxy-imide/Steel Joints - Influence of Environment on Creep Rate', The Journal of Adhesion, 68: 3, 281 — 300
To link to this Article: DOI: 10.1080/00218469808029259
URL: http://dx.doi.org/10.1080/00218469808029259

J. Adhesion, 1998, Vol. 68, pp. 281–300
Reprints available directly from the publisher
Photocopying permitted by license only

Creep Behaviour at High Temperature of Epoxy-imide/Steel Joints – Influence of Environment on Creep Rate

N. PICCIRELLI, Y. AURIAC and M. E. R. SHANAHAN*

Centre National de la Recherche Scientifique, Ecole Nationale Supérieure des Mines de Paris, Centre des Matériaux P.M. Fourt, B. P. 87, 91003 EVRY Cédex, France

(Received 12 November 1997; In final form 4 March 1998)

Torsional joints of stainless steel bonded with an epoxy-imide high-temperature structural adhesive have been tested in creep in the temperature range 180–245°C. After primary creep, in which creep rate decreases, there follows a period of secondary, or stationary, creep at constant creep rate, before failure occurs abruptly or after a period of tertiary creep with increasing deformation rate. Secondary creep has been analysed and two types of behaviour have been observed, each being attributed to a predominant mechanism: α at high stress and/or temperature, and β at low stress and/or temperature. Using reaction rate theory, a theoretical model has been developed in which the distinction between the processes is associated with a stress-activated transition temperature, closely related to the glass transition temperature. This transition evolves with creep. Creep in nitrogen is shown to be somewhat less marked than in air, suggesting synergy between stress and oxidation. Creep and ensuing degradation are essentially physical phenomena, yet the presence of oxygen can clearly exacerbate both.

Keywords: Creep; epoxy-imide; high-temperature; oxidation; rate process; steel; structural adhesive; torsion; transition

INTRODUCTION

The growing use of polymeric-matrix-based composite materials, particularly in the aerospace industry, clearly favours the use of

* Corresponding author.

adhesive bonding as an assembly technique. Bonding presents several advantages compared with traditional, mechanical methods, such as reduction in stress concentrations, weight saving, lesser problems of corrosion and/or fatigue. The use of structural components withstanding elevated service temperatures necessitates that adhesives of comparable heat resistance must be sought. Since most structural adhesives are designed to operate over long periods in their glassy state, basic materials are likely to be polymers of high glass transition temperature, T_g. Notwithstanding, combined effects of exposure time, environment and stress may lead to a reduction in mechanical performance of the adhesive and, amongst other problems, creep or time-dependent deformation.

The creep behaviour of adhesive assemblies has been the subject of various studies, but mechanical aspects form the major interest [1–7]. Relatively few studies would appear to have been undertaken concerning microstructural changes undergone by the adhesive during creep, due to the environment and applied load, although some environmental degradation effects have been noted [8, 9].

In the work reported here, we consider the creep behaviour of structural assemblies based on an epoxy-imide adhesive, and a stainless steel. We mainly consider effects of environment, temperature and stress level on the deformation rate corresponding to secondary, or steady-state creep. This corresponds essentially to the viscous character of the adhesive and, thus, may be related to macromolecular structure [10–12].

The temperature range studied is from 180 to 245°C, corresponding to the upper service temperature range of the polymer considered. Creep has been provoked both in air and in a nitrogen atmosphere, in order to monitor modifications in behaviour due to oxidation.

EXPERIMENTAL

Materials

The adhesive studied was an epoxy-imide resin, denoted FM32 and distributed by CYTEC. This adhesive is supported on a glass–fibre fabric intended to facilitate handling before cure.

The material used for substrates was a stainless steel denoted S321 containing 19% chromium, 13% nickel and 0.8% titanium, giving it good thermal properties and corrosion resistance. Although FM32 is often used with other substrates, choice of S321 for our study was partially governed by the fact that this steel presents purely elastic behaviour in the stress and temperature ranges under consideration. This is of considerable use in the interpretation of experimental results.

The steel underwent a simple pre-bonding surface treatment consisting of a trichloroethylene vapour decreasing and sand-blasting with 160 μm grade corundum, leading to an average surface roughness, R_a, of *ca.* 1.8 μm.

Crosslinking of bonded assemblies was effected by curing at 180°C for 4 hours under a pressure of 3 bars, followed by a post-cure at 205°C, also for 4 hours. Temperature increase and decrease rates from ambient were $3°C\,min^{-1}$. A DSC study of the material revealed that complete crosslinking is attained at 180°C and that the post-cure (recommended by the manufacturer) probably serves essentially to relieve any internal stresses.

Creep Tests

The test geometry adopted for creep tests was that known as the "Napkin Ring", initially suggested by de Bruyne [13] and later developed by various workers [14–17]. Two hollowed-out cylindrical substrates, of external and internal radii denoted r_e and r_i, respectively, of 9.75 and 7 mm, and length 40 mm, are bonded end to end using a ring of the adhesive FM32 of thickness, e, equal to 1.2 ± 0.1 mm (see Fig. 1). The radii were chosen to represent a practical compromise between a sufficiently low value of the ratio $(r_e - r_i)/r_e$ (to ensure a homogeneous stress distribution) and the feasibility of producing well-constructed joints. The dimensions chosen are such that shear stress varies relatively little along the cylindrical radius from r_i to r_e, even under elastic conditions. Similarly, the thickness of the adhesive layer is sufficient to obtain reproducible results without obscuring any potential effects related to the interphase.

"Napkin Ring" joints were constructed using a special jig, made in the laboratory, ensuring accurate alignment of the axes of the two bonded cylinders. Joint thickness was assured by using several layers

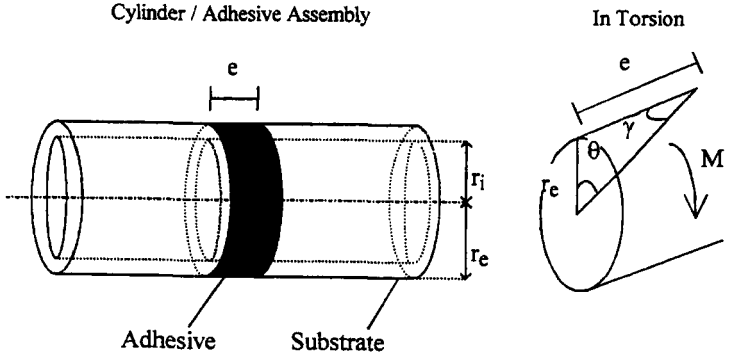

FIGURE 1 Schematic representation of the "Napkin-Ring" geometry used for torsional creep tests.

of adhesive film (4, leading to a joint thickness of 1.2 mm). Gaskets of polytetrafluoroethylene (PTFE) were placed both inside and around the assemblies before cure to prevent adhesive leak during crosslinking and the formation of fillets, modifying stress distributions.

Adhesive assemblies were loaded in torsion using a machine specially developed for this geometry (see Fig. 2). A lever arm allows application of a couple, M, whilst the attachment jaws are free to slide along the joint's cylindrical axis as a measure to prevent dilational or tensile stresses in the adhesive joint during creep.

Couple M was controlled by varying the dead loads attached to the lever arm, whilst rotation in the joint was monitored using an LVDT extensometer. The relative linear displacement, $\delta(t)$, measured at the extremities of two bars, one attached to each steel cylinder, was followed as a function of time, t, using a PC, and the corresponding rotation, $\theta(t)$, calculated from the simple formula assuming θ small (see Fig. 1):

$$\tan\theta(t) \approx \theta(t) \approx \delta(t)/L \tag{1}$$

where L is the radial distance from the cylindrical axis to the point of measurement of the LVDT.

The measurement bars, being attached to each cylinder at a distance, d, from the steel/adhesive interface, also rotate relative to each other under applied load partly because of shear strain in the steel

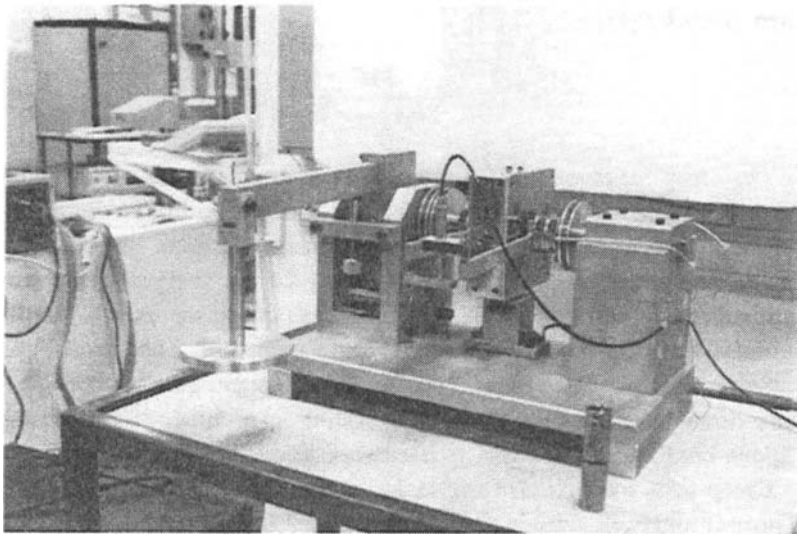

FIGURE 2 Torsional creep machine constructed to test cylindrical adhesive joints at elevated temperatures.

and not just in the adhesive. Allowance for strain in the steel was made and the contribution to $\theta(t)$ then deducted in order to obtain the rotation occurring only in the joint itself, θ_a, [17]. Since the substrate is purely elastic in the conditions studied, its contribution is time-independent and inversely proportional to $G_s(T)$, its shear modulus (function of temperature, T). We can, thus, calculate shear strain, $\gamma(t)$, of the adhesive only as a function of time from the following expressions [18]:

$$\theta_a(t) = \theta(t) - \frac{4Md}{\pi(r_e^4 - r_i^4)G_s(T)} \tag{2}$$

$$\gamma(t) \approx \frac{\theta_a(t)r_e}{e} \tag{3}$$

In the above equations, it is assumed that residual stresses are negligible, as should be the case given the post-cure treatment undergone by the adhesive joints (see above).

Under conditions of creep, plastic behaviour of the adhesive may reasonably be assumed. The shear stress, τ, (independent of radius) is

then given by [19]:

$$\tau = \frac{3M}{2\pi(r_e^3 - r_i^3)} \tag{4}$$

The creep machine was equipped with a circular oven of diameter 25 mm and length 40 mm in order to heat the adhesive joint. In addition, a heating element was placed inside the joint assembly, in order to minimise thermal gradients. Creep temperature was controlled to within ± 1°C. A thermal stabilisation period of 30 minutes was observed before submitting a joint to applied load.

Some experiments were carried out in a nitrogen atmosphere. This was done by enclosing the whole system in a nitrogen-containing "glove box" before heating to test temperature.

Creep tests were carried out in air at 180, 200, 215, 230 and 245°C. Those in nitrogen were mainly limited to 200 and 215°C.

RESULTS AND DISCUSSION

In Figures 3 to 7, we present creep curves as $\gamma(t)$ *vs* t obtained at temperatures from 180 to 245°C. The main figures are on a logarithmic time scale, whereas insets show a linear time scale. In most cases, tests have been taken to joint failure. Lower temperatures and/or higher stresses tend to lead to a fairly abrupt failure as seen on a $\gamma(t)$ *vs* t plot. However, under conditions of higher temperatures and low applied loads, there is a tendency for creep rate to increase, giving a period of tertiary creep preceding failure. Apart from this difference, creep under the various temperature and stress conditions studied leads to similar symptoms: an initial period of decreasing creep rate (primary creep) is followed by secondary, or stationary, creep in which creep rate remains constant and resembles viscous flow. The gradients of the secondary creep periods in Figures 3 to 7, corresponding to creep rate, or speed, will be analysed below. When secondary creep has been attained, we consider that the purely elastic component of strain has reached equilibrium (for the stress level in question) and that the time-dependent behaviour of the adhesive may be treated as if due to viscous effects. We have considered creep rate in the secondary zone as

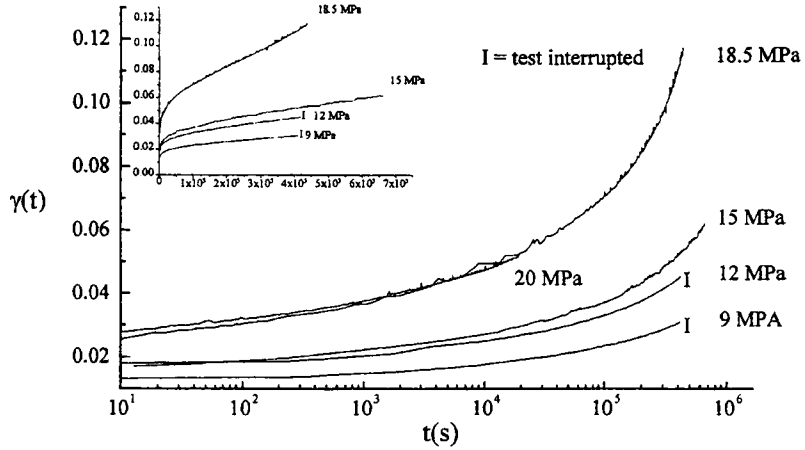

FIGURE 3 Creep behaviour of joints at 180°C in air at various stresses. Strain, $\gamma(t)$, *vs* time, t, on a logarithmic scale. Inset corresponds to time on a linear scale.

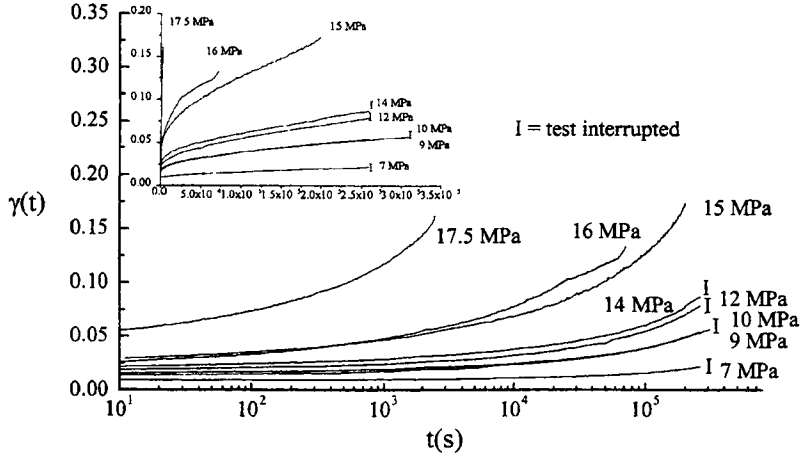

FIGURE 4 As for Figure 3, but temperature 200°C.

a function of stress and temperature, these data suggesting mechanisms of microstructural evolution [10–12].

Secondary Creep Rate in Air

We have determined creep rate in the secondary phase by representing the evolution of creep rate, $\dot{\gamma}\,(= d\gamma/dt)$, as a function of creep strain,

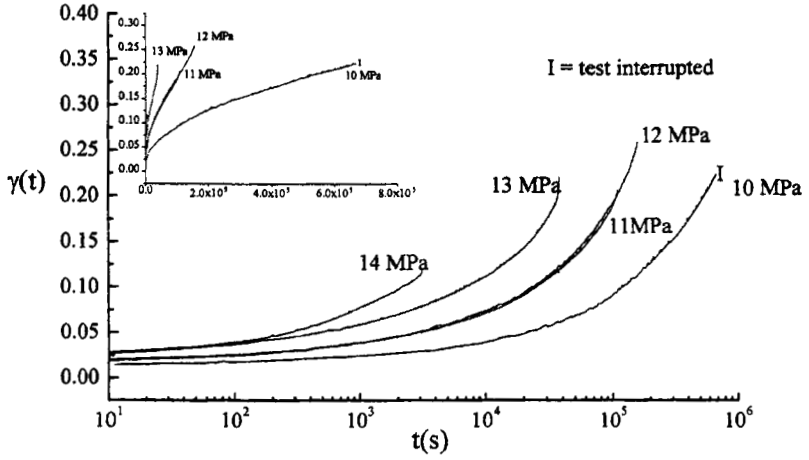

FIGURE 5 As for Figure 3, but temperature 215°C.

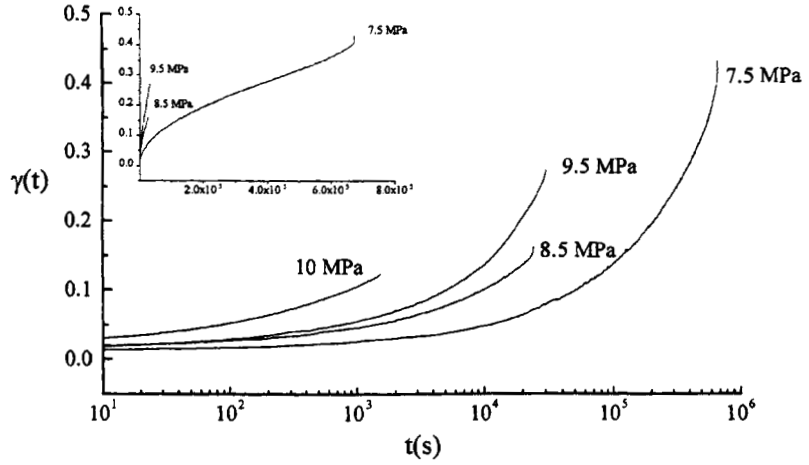

FIGURE 6 As for Figure 3, but temperature 230°C.

γ, in the manner of Sherby and Dorn [20]. Secondary creep is characterised by a horizontal plateau of which the ordinate corresponds to $\dot{\gamma}$(sec) (see example of Fig. 8). Secondary creep rates for the various conditions of applied stress, τ, and temperature are presented in Figure 9. On this plot of $\log \dot{\gamma}$(sec) *vs* τ, covering five temperatures, two distinct zones may be recognised, depending on stress and

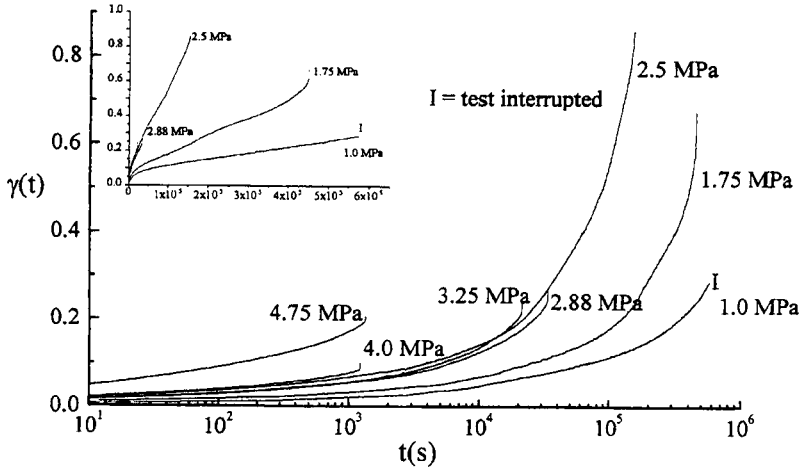

FIGURE 7 As for Figure 3, but temperature 245°C.

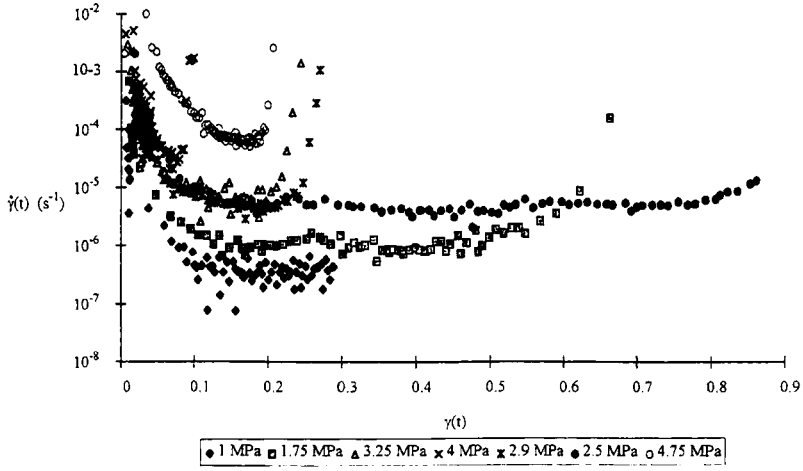

FIGURE 8 Creep rate, $\dot{\gamma}(t)$, *vs* strain, $\gamma(t)$ at 245°C for various applied stresses: plateaus represent secondary creep.

temperature. At low temperatures (180 and 200°C) and for (relatively) low stresses, $\dot{\gamma}$(sec), although increasing with τ, is only mildly stress-dependent. However, at higher stresses and/or temperatures the gradient of $\log \dot{\gamma}(\text{sec})$ *vs* τ increases, showing more sensitive stress-dependent exponential behaviour. The overall appearance of Figure 9

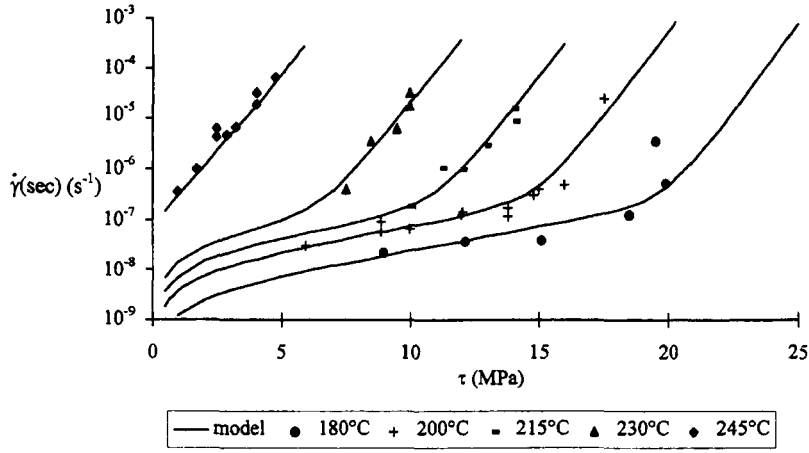

FIGURE 9 Evolution of secondary creep rate, $\dot{\gamma}$(sec), with applied stress, τ, in air at various temperatures.

suggests the presence of two mechanisms governing secondary creep behaviour, although not all combinations of stress and temperature were experimentally accessible.

Various studies of polymeric creep have shown it to be possible to relate the evolution of creep rate in the secondary creep domain, $\dot{\gamma}$(sec) to applied stress, τ, using the generalised theory of Ree–Eyring [10–12, 21]:

$$\dot{\gamma}(\text{sec}) = \sum_{i=1}^{n} \dot{\gamma}_{oi} \exp\left[-\frac{\Delta H_i}{RT}\right] \sinh\left[\frac{v_i \tau}{RT}\right] \tag{5}$$

where ΔH_i is the enthalpy of activation associated with process i, v_i is the activation volume of mechanism i, τ is applied stress (calculated from Eq. (4) for our purposes), R and T are, respectively, the gas constant and (absolute) creep temperature, and $\dot{\gamma}_{oi}$ are constants.

This expression relates viscous behaviour to molecular chain motion. The summation allows for the existence of several mechanisms activated by stress and temperature. Our experimental results suggest the presence of two mechanisms:

- at high temperature and/or stress, mechanism α predominates and is characterised by activation enthalpy ΔH_α and volume v_α,

– at low temperature and/or stress, mechanism β predominates with corresponding parameters ΔH_β and v_β. The latter mechanism triggers easier, or less constrained, chain motion which corresponds to the major deformation mode at low temperature. A recent study on an epoxy adhesive attributes this mode to the motion of local molecular groups, being visible above the β transition of the polymer [22].

Assuming two predominant mechanisms as described above, regression analysis has been applied to the experimental values shown in Figure 9, employing Eq. (5) as the basic equation ($n = 2$). Table I summarises the values of the parameters thus obtained.

Mechanism α is associated with an activation enthalpy of the same order of magnitude as that corresponding to the glass transition of the polymer [23] (*ca.* 943 kJ mole^{-1}). We therefore infer that the molecular chain motions intervening at high stress implicate mainly principal macromolecular chain segments over long distances. These movements are principally activated above the glass transition of the material. Conversely, the "softer" mechanism β comes into play at low applied stress, corresponding to a lower energy and relatively short range molecular motion.

At lower temperatures, the macromolecular structure of the adhesive is relatively rigid: long range chain motion is hindered. There remain short-range motion and the movement of local molecular groups: strain rate evolves slowly with applied stress. As the temperature increases, approaching the glass transition, viscous behaviour of the polymer increases. With the increased freedom of the macromolecular chains, long-range motion is facilitated and, thus, variation of applied stress has a more significant effect on creep rate.

The major mechanism at 180 and 200°C has an activation enthalpy of 92 kJ mole^{-1}. This value is much greater than that corresponding to

TABLE I Values of the parameters calculated for Eq. (5) (with $n = 2$), when applied to experimental data shown in Figure 9

	Mechanism, i	
	α	β
Activation enthalpy, ΔH_i (kJ mole^{-1})	974	92
Activation volume, v_i (m^3 mole^{-1})	5.9×10^{-3}	8.5×10^{-4}
$\ell n(\dot{\gamma}_{oi})$ ($\ell n(s^{-1})$)	209	5.6

the β transition [23] (*ca.* 44 kJ mole^{-1}). It may be inferred that corresponding chain movements are more consequential than those related to the β transition alone. We may, therefore, postulate that low stress (and/or temperature) creep is due to a mixture of β and glass-transition-type behaviour. This hypothesis gains support from work done some years ago by Roetling [24, 25]. Roetling showed that strain rate was governed by a mixed process when the test temperature was slightly lower than that corresponding to the glass transition.

An increase in creep temperature can facilitate the α mode of deformation for a *reduced* applied stress. We have, therefore, considered the evolution of secondary creep rate as a function of temperature for constant stress.

Temperature Effects on Secondary Creep Rate

In Figure 10, we present secondary strain rate, $\dot{\gamma}$(sec), as a function of test temperature, for three levels of applied stress, τ, equal to 9, 12 and 14 MPa. Experimental results are accompanied by curves calculated by applying Eq. (5) ($n = 2$). Despite the small number of experimental points, particularly at high temperature, the presence of mechanisms α and β can be observed, respectively being predominant at high and low

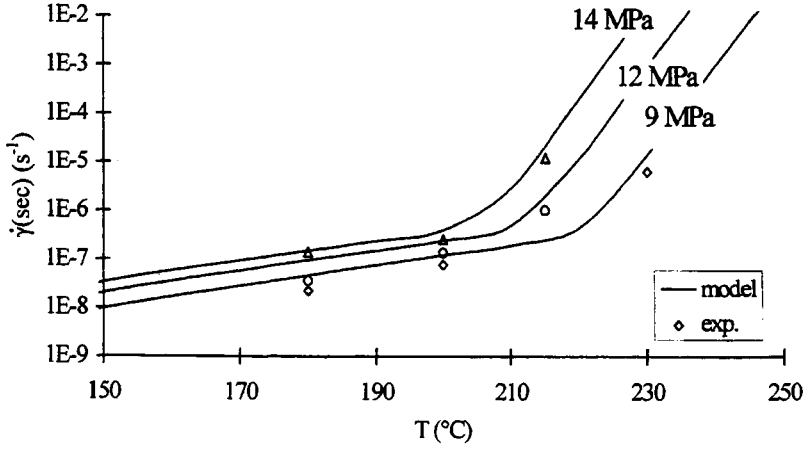

FIGURE 10 Secondary creep rate, $\dot{\gamma}$(sec), *vs* temperature, for various stress levels.

temperatures. The transition zone between α and β decreases in temperature as the stress increases. We may (albeit slightly artificially) define a transition temperature, T_t, at the intersection of the lines of different gradient of Figure 10, corresponding to each stress level. This transition temperature, T_t, separating the two processes α and β, decreases linearly with increasing stress level, τ, and may be considered to be the limiting temperature, above which creep strain becomes significant in air, for a given stress.

Using Eq. (5), we have simulated the evolution of T_t during creep as a function of applied stress. We assume that mechanisms α and β are of equal importance at T_t. Allowing the simplification:

$$\sinh\left[\frac{v\tau}{RT}\right] \approx \frac{1}{2}\exp\left[\frac{v\tau}{RT}\right] \tag{6}$$

for $\tau > 2\,\text{MPa}$, we obtain:

$$T_t = \frac{[(\Delta H_\alpha - \Delta H_\beta) + (v_\beta - v_\alpha)\tau]}{R \cdot \ell n[(\dot{\gamma}_{o\alpha}/\dot{\gamma}_{o\beta})]} \tag{7}$$

If τ is very small, we may use the approximation:

$$\sinh\left[\frac{v\tau}{RT}\right] \approx \frac{v\tau}{RT} \tag{8}$$

in which case:

$$T_t = \frac{(\Delta H_\alpha - \Delta H_\beta)}{R \cdot \ell n[(v_\alpha \dot{\gamma}_{o\alpha}/v_\beta \dot{\gamma}_{o\beta})]} \tag{9}$$

From Eq. (9) and the values given in Table I, we may calculate the value of T_t extrapolated to zero stress and obtain 243°C.

The diagram of Figure 11 was constructed from the above equations and shows the stress/temperature zones in which either mechanism α or mechanism β predominates in secondary creep, the dividing line corresponding to T_t. The outer envelope corresponds to maximum joint strength (normal test to failure, without creep) and serves to limit

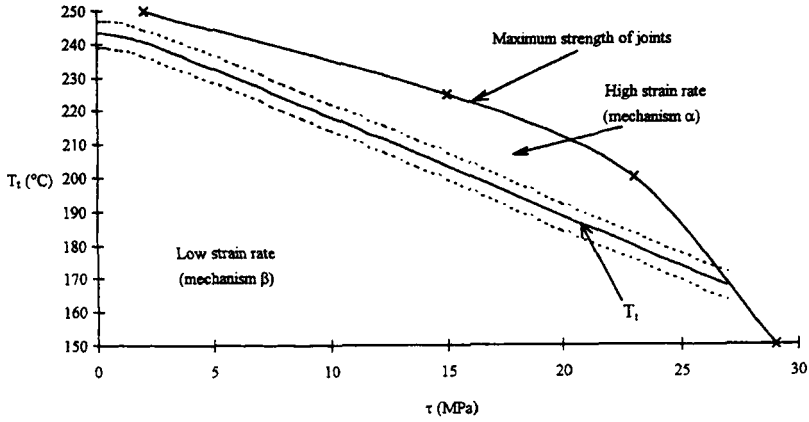

FIGURE 11 Diagram constructed from theory and calculated parameters giving stress/temperature zones corresponding to secondary creep controlled mainly by mechanism α or by mechanism β (see text for details).

T_t at high stresses when failure occurs instantaneously before the onset of creep behaviour. Above 243°C, only mechanism α may dominate.

The glass transition temperature, T_g, of this epoxy-imide, as found by viscoelastometry, is 275°C at a frequency of 5 Hz and 252°C at a frequency of 10^{-3} Hz, the latter frequency being more representative of creep conditions. The proximity of these values to the theoretical T_t of 243°C discussed above suggests their equivalence: T_t may thus be reasonably assimilated to the glass transition. Above 243°C, we exceed the effective T_g of the polymer whatever the applied load and, thus, only one secondary creep mechanism may be observed. Below 243°C, the application of a sufficiently high stress activates creep mechanism α.

The decrease of T_t and, by hypothesis, T_g, of the polymer may be associated with degradation of the macromolecular network under the combined effects of temperature, stress and local environment. Applied stress favours the process of thermo-oxidation [23] and leads to the scission of chemical bonds and, therefore, the reduction of T_g during creep.

The influence of the local environment on creep has been studied and is discussed below.

Effects of Oxygen-Creep in Nitrogen

Some creep tests have been performed in a nitrogen atmosphere at 200 and 215°C. For these temperatures, both mechanisms α and β are visible at high stresses in an air atmosphere. Figures 12 and 13 present creep curves at (relatively) high and low stresses, both in air and in nitrogen.

When the stress is low, the atmosphere has little influence on creep behaviour: creep curves are reasonably similar. However, when the stress is higher, creep is more significant in air. As for air, we have considered secondary creep rates in nitrogen. Figure 14 shows the combined results, corresponding both to creep in air and in nitrogen.

Creep curves in nitrogen appear to be reasonably parallel (at the lower temperatures) and, in addition, their gradient seems reasonably close to, although higher than, that of the curves in air corresponding to mechanism β. Using Eq. (5) ($n = 1$), we have evaluated the parameters ΔH, v and $\ell n(\dot{\gamma}_o)$, given in Table II.

For high stresses, secondary creep rate is lower in nitrogen than in air. Nevertheless, a modification to the creep mechanism is manifest since the activation enthalpy in nitrogen is higher than ΔH_β. We, therefore, suggest a physical evolution of the mechanism(s) governing creep due simply to the increase in stress. The considerably higher creep rates obtained in air in the same stress range as the tests in nitrogen, as shown in Figure 14, strongly suggest a synergistic effect of the combination of applied stress and atmospheric oxygen. Oxidation of the adhesive seems to be favoured by the application of stress. Indeed, the higher gradient in air is compatible with a higher oxidation rate accompanying a higher stress level. It would seem reasonable to assume that deformation of the macromolecular network leads to the scission of some macromolecular chains and the creation of free radicals capable of reacting with the atmospheric oxygen, thus accelerating the process of thermal oxidation. This degradation could provoke the scission of other chains in the bulk polymer, due to higher local stresses, thus leading to an overall, effective reduction in crosslink density. Thermal degradation would, thus, increase the freedom of movement of chains leading to a higher creep rate. As a result T_g would be reduced [23].

By contrast, when the applied stress is low, thermal-oxidation depends only on the ageing of the adhesive directly exposed to oxygen,

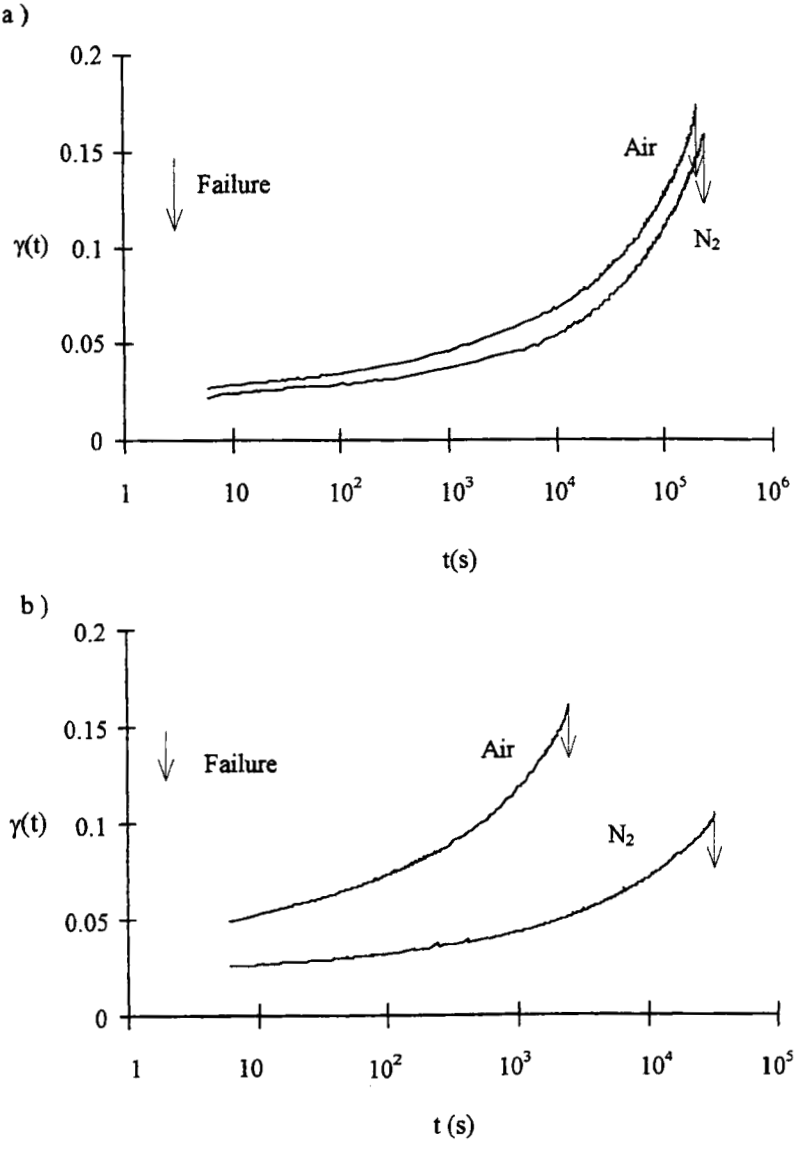

FIGURE 12 Creep of torsional joints in air and in nitrogen at 200°C. (a) $\tau = 15$ MPa, (b) $\tau = 17.5$ MPa.

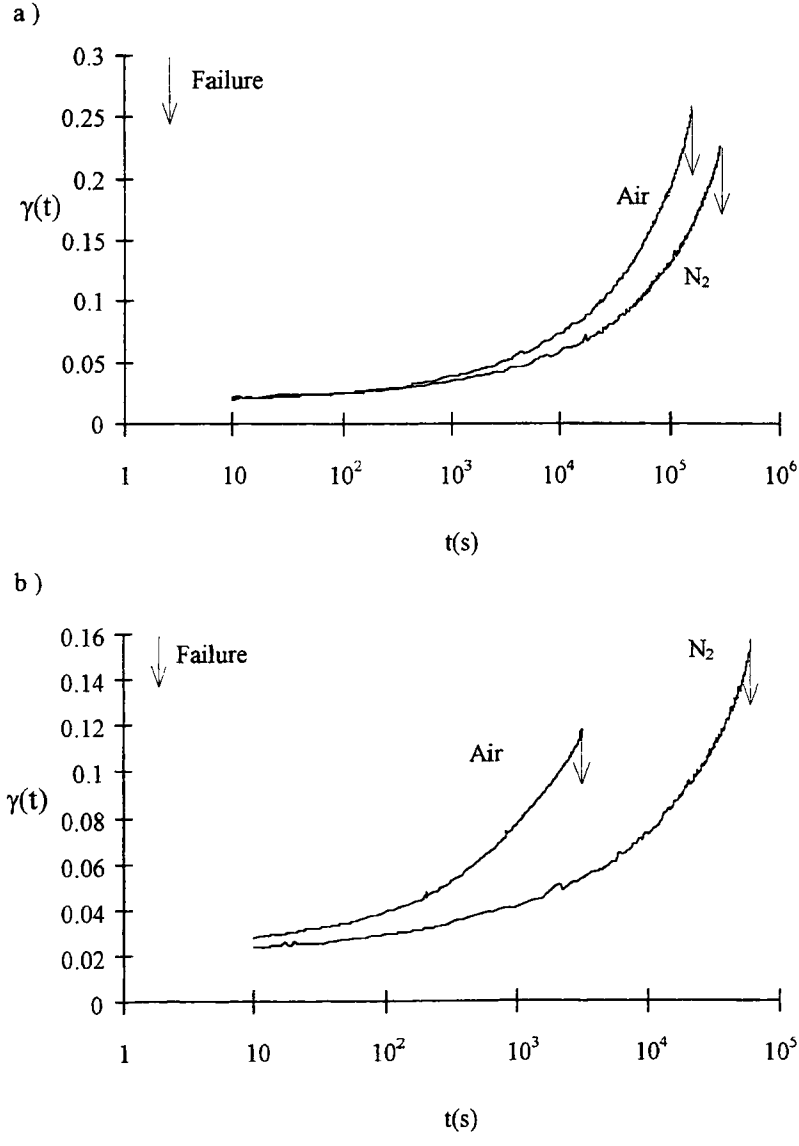

FIGURE 13 As for Figure 12, but temperature 215°C.

this effect being relatively slow at 200 and 215°C [23]. Thus, under these conditions, chemical modification of the polymer is limited and the nature of the environment less significant.

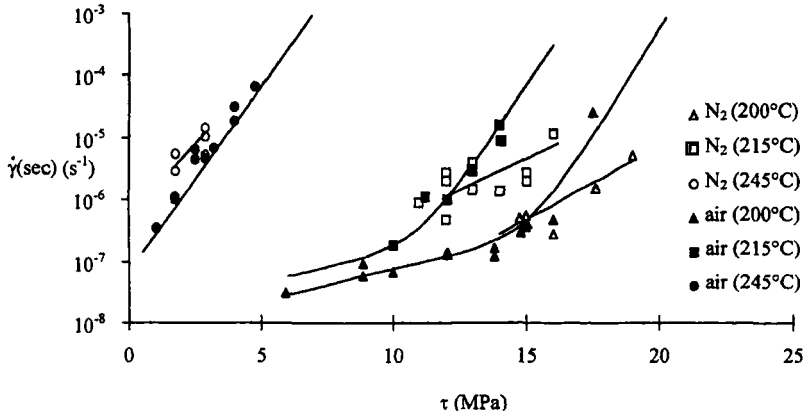

FIGURE 14 Evolution of secondary creep rate, $\dot{\gamma}$(sec), with applied stress, τ, in air and nitrogen at various temperatures.

TABLE II Values of parameters calculated for Eq. (5) (with $n = 1$) for secondary creep in nitrogen

Activation enthalpy, ΔH (kJ mole^{-1})	347
Activation volume, v (m^3 mole^{-1})	1.8×10^{-3}
$\ell n(\dot{\gamma}_o)(\ell n(s^{-1}))$	67.5

When the creep temperature is equal or superior to T_g, oxidation of the polymeric network becomes clear from a significant increase in creep rate with increasing stress.

Although a purely physical phenomenon may be at the origin of a reduced T_g following creep, effects may be exacerbated by oxidation.

CONCLUSIONS

The creep behaviour of torsional joints made from an epoxy-imide adhesive and a stainless steel has been studied at elevated temperatures (180–245°C). Secondary creep rate of these structures, when in air, is principally governed by two molecular mechanisms, which may be compared with the glass transition and the β transition of the polymer. We have demonstrated the existence of an effective transition temperature between the two mechanisms, which decreases as applied stress increases. This transition may be assimilated to T_g.

During creep, the epoxy-imide polymer undergoes oxidation in air, favoured by temperature and stress level. Degradation would appear to lead to an effective reduction in crosslink density and a decrease in T_g. In turn, long-range molecular motion is favoured, leading to an increase in creep rate, particularly under high stress. A theoretical model has been suggested leading to a diagram (Fig. 11) giving the possible service limits of the adhesive as a function of applied stress. Thus, for a given temperature, as long as the applied stress is sufficiently low, the oxidation process remains slow and creep rates remain low.

Acknowledgements

We thank the Société Nationale d'Etude et de Construction de Moteurs d'Aviation (S.N.E.C.M.A.) for their financial and material support in this study.

References

[1] Allen, K. W. and Shanahan, M. E. R., *J. Adhesion* **7**, 161 (1975).
[2] Allen, K. W. and Shanahan, M. E. R., *J. Adhesion* **8**, 43 (1976).
[3] Althof, W., *J. Reinf. Plast. Comp.* **1**, 29 (1982).
[4] Brinson, H. F., *Composites* **13**(4), 377 (1982).
[5] Brinson, H. F., Composite Structures, Ed. Elsevier Applied Science, Vol. 3 (1985), p. 1.
[6] Sancaktar, E., in: *Eng. Mat. Hand.*, Vol. 3, "Adhesives and Sealants" (ASM Int., Metals Park, OH, 1990), p. 349.
[7] Magnery, L. A. and Shapery, R. A., *J. Adhesion* **34**, 17 (1991).
[8] Fay, P., Adhesion 1990, *Fourth International Conference at the University of Cambridge*, p. 25/1.
[9] Springer, G. S. and Wang, T. K., *J. Reinf. Plast. Comp.* **4**, 215 (1985).
[10] Bauwens-Crowet, C. and Bauwens, J. C., *J. Mat. Sci.* **10**, 1779 (1975).
[11] Ward, I. M. and Wilding, M. A., *J. Polym. Sci. Phys. Ed.* **22**, 561 (1984).
[12] Rasburn, J., Klein, P. G. and Ward, I. M., *J. Polym. Sci. Phys. Ed.* **32**, 1329 (1994).
[13] de Bruyne, N. A., in: *Adhesion and Adhesives*, de Bruyne, N. A. and Houwink, R., Eds., Amsterdam (Elsevier, 1951), p. 91.
[14] Gillespie, T. and Rideal, E., *J. Colloid Sci.* **11**, 732 (1956).
[15] Foulkes, H. and Wake, W. C., *J. Adhesion* **2**, 254 (1970).
[16] De' Nève, B. and Shanahan, M. E. R., *Int. J. Adhesion Adhesives* **12**, 191 (1992).
[17] Zanni-Deffarges, M. P. and Shanahan, M. E. R., *Int. J. Adhesion Adhesives* **13**, 41 (1993).
[18] Adams, R. D. and Wake, W. C., *Structural Adhesive Joints in Engineering* (Elsevier Applied Science, London, 1986).
[19] Kinloch, A. J., *Adhesion and Adhesives* (Chapman and Hall, London, 1987).
[20] Sherby, O. D. and Dorn, J. E., *J. Mech. Phys. Sol.* **6**, 145 (1958).

[21] Ree, T. and Eyring, H., *J. Appl. Phys.* **26**(7), 793 (1955).
[22] Cayssials, F. and Lataillade, J. L., *J. Adhesion* **58**, 281 (1996).
[23] Piccirelli, N., *Ph. D. Thesis*, ENSM Paris (1997).
[24] Roetling, J. A., *Polymer* **6**, 615 (1965).
[25] Roetling, J. A., *Polymer* **7**, 303 (1966).